

# Resonance Raman Excitation Profiles Indicate Multiple Cys → Cu Charge Transfer Transitions in Type 1 Copper Proteins

Jane Han,<sup>1a</sup> Thomas M. Loehr,<sup>1a</sup> Yi Lu,<sup>1b</sup> Joan Selverstone Valentine,<sup>1b</sup>  
Bruce A. Averill,<sup>1c</sup> and Joann Sanders-Loehr<sup>\*,1a</sup>

Contribution from the Department of Chemical and Biological Sciences, Oregon Graduate Institute of Science and Technology, Beaverton, Oregon 97006-1999, Department of Chemistry and Biochemistry, University of California, Los Angeles, California 90024, and Department of Chemistry, University of Virginia, Charlottesville, Virginia 22901

Received July 30, 1992

**Abstract:** Nitrite reductase (NiR) from *Achromobacter cycloclastes* and mutant yeast Cu-Zn superoxide dismutase (with Cys substituted for His80 and Cu for Zn) have both been shown to contain type 1 Cu sites. However, they differ from other type 1 (blue) Cu proteins in that they are green: the absorption band at ~460 nm is more intense than the one at ~600 nm. Excitation within either of these absorption bands leads to resonance Raman (RR) spectra that are characteristic of type 1 Cu with a large number of peaks between 250 and 500 cm<sup>-1</sup>. The RR spectra of NiR and mutant SOD are thus indicative of a Cu-cysteinate chromophore with a short Cu-S bond distance (~2.1 Å) and a coplanar cysteine moiety (Cu-S<sub>γ</sub>-C<sub>β</sub>-C<sub>α</sub> dihedral angle ~180°). Since excitation within either the 460- or the 600-nm absorption band leads to a similar RR spectrum, both electronic transitions are likely to have (Cys)S → Cu(II) CT character. The RR enhancement profiles for azurin and pseudoazurin indicate that their low-intensity 460-nm absorption bands also have a Cys → Cu CT component. The occurrence of two different copper-cysteinate transitions at 460 and 600 nm helps to explain the fact that, although their relative absorptivities vary, the sum of ε<sub>460</sub> and ε<sub>600</sub> is fairly constant. Increased intensity at 460 nm appears to be associated with stronger binding of the axial ligand and a concomitant shift from a trigonal planar toward a more tetrahedral Cu site geometry.

## Introduction

Type 1 (blue) copper sites are found in both mononuclear and multinuclear copper proteins where their most common function is the catalysis of inter- and intramolecular electron transfer, respectively.<sup>2</sup> X-ray crystal structure determinations for seven different proteins (three plastocyanins, azurin, pseudoazurin, basic blue protein, and ascorbate oxidase) reveal a highly conserved site with the copper coordinated to one cysteine and two histidines in a nearly trigonal-planar array.<sup>2</sup> This unusual trigonal-pyramidal geometry includes a short Cu-S(Cys) at a distance of 2.12 ± 0.05 Å and an axial methionine at a considerably longer distance of 2.6–3.1 Å.<sup>3</sup>

Another striking feature of the type 1 Cu site is its intense absorption (ε > 3000 M<sup>-1</sup> cm<sup>-1</sup>) near 600 nm.<sup>4,5</sup> In a recent study of plastocyanin, Gewirth and Solomon<sup>6</sup> proposed detailed assignments of the entire electronic spectrum. The dominant band at 600 nm was ascribed to a charge-transfer transition from the cysteine S pπ orbital to the d<sub>x<sup>2</sup>-y<sup>2</sup></sub> orbital of Cu(II), with the large intensity deriving from the excellent overlap between ground- and excited-state wave functions. An unresolved band at 535 nm was ascribed to a transition involving pseudo-σ overlap between a cysteine S p orbital and a Cu d orbital. Two weak features at 430 and 465 nm were attributed to Met → Cu(II) and His → Cu(II) CT, respectively. Finally, the four absorption bands at lower energy (between 650 and 1050 nm) were assigned to ligand-field transitions, particularly on the basis of their MCD behavior.

This analysis revealed that the Cu(II)-thiolate interaction dominates the electronic spectrum, leading to the possibility of multiple (Cys)S → Cu(II) CT transitions and the probable contribution of Cu ligands to a number of different absorption bands.

An anomalous electronic spectrum is associated with the type 1 Cu site of nitrite reductase (NiR) from *Achromobacter cycloclastes*.<sup>7,8</sup> According to the X-ray crystal structure, the protein has a typical type 1 Cu site with a His<sub>2</sub>Cys trigonal-planar ligand set which functions to transfer electrons to a type 2 Cu, 12.5 Å away.<sup>9</sup> The type 2 Cu site appears to be responsible for the reduction of NO<sub>2</sub><sup>-</sup> to NO or N<sub>2</sub>O.<sup>9,10</sup> In the absorption spectrum of NiR, the most intense feature occurs at 458 nm (ε = 2530 M<sup>-1</sup> cm<sup>-1</sup>) with additional prominent bands at 385, 585, and 695 nm. This spectrum is unaltered in protein samples that are deficient in type 2 copper.<sup>11</sup> Despite the unusual electronic spectrum associated with the NiR copper site, its EPR and resonance Raman (RR) spectra are otherwise characteristic of a type 1 Cu.<sup>11,12</sup>

A similarly unusual electronic spectrum is observed for a mutant of Cu<sub>2</sub>Zn<sub>2</sub>-superoxide dismutase (SOD) from *Saccharomyces cerevisiae*. In the native yeast protein, the tetragonal type 2 Cu appears to be coordinated to four His, one of which bridges through imidazolate to a tetrahedral Zn having two other His and one Asp as ligands (Scheme I).<sup>13,14</sup> Mutation of His 80 in the zinc

(1) (a) Oregon Graduate Institute of Science and Technology. (b) University of California, Los Angeles. (c) University of Virginia.

(2) Adman, E. T. *Adv. Protein Chem.* **1991**, *42*, 145-197.

(3) Han, J.; Adman, E. T.; Beppu, T.; Codd, R.; Freeman, H. C.; Huq, L.; Loehr, T. M.; Sanders-Loehr, J. *Biochemistry* **1991**, *30*, 10 904-10 913.

(4) Adman, E. T. In *Metalloproteins*; Harrison, P., Ed.; Verlag Chemie: Weinheim, FRG, 1985; Part I, pp 1-42.

(5) (a) Solomon, E. I.; Baldwin, M. J.; Lowery, M. D. *Chem. Rev.* **1992**, *92*, 521-542. (b) Penfield, K. W.; Gay, R. R.; Himmelwright, R. S.; Eickman, N. C.; Norris, V. A.; Freeman, H. C.; Solomon, E. I. *J. Am. Chem. Soc.* **1981**, *103*, 4382-4388.

(6) Gewirth, A. A.; Solomon, E. I. *J. Am. Chem. Soc.* **1988**, *110*, 3811-3819.

(7) Iwasaki, H.; Matsubara, T. *J. Biochem. (Tokyo)* **1972**, *71*, 645-652.

(8) Liu, M.-Y.; Liu, M.-C.; Payne, W.; LeGall, J. *J. Bacteriol.* **1986**, *166*, 604-608.

(9) Godden, J. W.; Turley, S.; Teller, D. C.; Adman, E. T.; Liu, M. Y.; Payne, W. J.; LeGall, J. *Science* **1991**, *253*, 438-442.

(10) Hulse, C. L.; Tiedje, J. M.; Averill, B. A. *Anal. Biochem.* **1988**, *172*, 420-426.

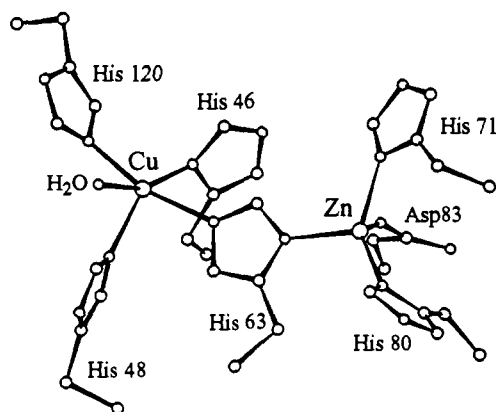
(11) Libby, E.; Averill, B. A. *Biochem. Biophys. Res. Commun.* **1992**, *187*, 1529-1535.

(12) Dooley, D. M.; Moog, R. S.; Liu, M.-Y.; Payne, W. J.; LeGall, J. *J. Biol. Chem.* **1988**, *263*, 14 625-14 628.

(13) Getzoff, E. D.; Tainer, J. A.; Weiner, P. K.; Kollman, P. A.; Richardson, J. S.; Richardson, D. C. *Nature (London)* **1983**, *306*, 287-290.

(14) Valentine, J. S.; Pantoliano, M. W. In *Copper Proteins*; Spiro, T. G., Ed.; Wiley: New York, 1981; pp 291-357.

Scheme I



site to Cys and replacement of Zn by Cu create a type 1 Cu site in H80C-Cu<sub>2</sub>Cu<sub>2</sub>SOD, based on its absorption and EPR spectra.<sup>15</sup> Like NiR, the mutant SOD has several intense CT bands with the strongest occurring at 459 nm ( $\epsilon \geq 1460 \text{ M}^{-1} \text{ cm}^{-1}$ ) and a somewhat weaker one at 595 nm ( $\epsilon \geq 1420 \text{ M}^{-1} \text{ cm}^{-1}$ ).<sup>16</sup>

To gain more information about these type 1 Cu sites and to understand the diversity of their absorption spectra, we have undertaken a study of their RR spectra and enhancement profiles. The RR spectra of type 1 Cu proteins exhibit as many as nine resonance-enhanced vibrational fundamentals between 330 and 490  $\text{cm}^{-1}$ .<sup>17,18</sup> The multiplicity of spectral features is believed to be due to a kinematic coupling of the Cu-S(Cys) stretch with vibrational motions of the cysteine and histidine ligands. Such coupling, particularly with cysteine ligand deformations, is enhanced by the coplanarity of the Cu-S bond with the C <sub>$\beta$</sub> , C <sub>$\alpha$</sub> , and N atoms of the cysteine moiety.<sup>3</sup> All of the RR modes show a maximum in intensity as the excitation wavelength approaches 600 nm, indicating that the Raman enhancement is derived from vibronic coupling with the principal (Cys)S  $\rightarrow$  Cu(II) CT transition.<sup>19,20</sup>

We have found that the RR spectra of NiR and mutant SOD (Cu<sub>2</sub>Cu<sub>2</sub>H80C) are similar to those of other type 1 Cu proteins. This observation implies the presence of a coplanar cysteinyl ligand with a Cu-S <sub>$\gamma$</sub> -C <sub>$\beta$</sub> -C <sub>$\alpha$</sub>  dihedral angle close to 180° in these proteins. In addition, the same set of vibrational modes is enhanced by excitation within either the 460- or 600-nm bands, indicating that both absorption bands have substantial (Cys)S  $\rightarrow$  Cu(II) CT character. A careful investigation of the enhancement behavior of two other type 1 Cu proteins, azurin and pseudoazurin, reveals that the electronic transitions in the 460-nm region, although weaker, also contain a substantial contribution from a Cu-cysteinyl chromophore. Thus, the 460-nm absorption in type 1 copper proteins is likely to have Cys  $\rightarrow$  Cu(II) CT character in addition to the previously assigned His  $\rightarrow$  Cu(II) CT.<sup>6</sup>

## Experimental Procedures

**Protein Samples.** Azurin from *Alcaligenes denitrificans* was obtained from a cloned *azu* gene expressed in *Escherichia coli*<sup>21</sup> and was the gift

of Dr. Gerard Canters and Carla Hoitink. Pseudoazurin from *Alcaligenes faecalis* S-622 was the gift of Dr. Teruhiko Beppu. Nitrite reductase from *Achromobacter cycloclastes* was purified in its native and type-2-depleted forms as described previously.<sup>11</sup> The H80C mutant of yeast superoxide dismutase was prepared in the apo form and reconstituted with 4 equiv of copper (in both the Cu and Zn sites) to yield Cu<sub>2</sub>Cu<sub>2</sub>-H80C.<sup>15,23</sup>

**Resonance Raman Spectroscopy.** Raman spectra were obtained on a Jarrell-Ash 25-300 spectrophotometer, equipped with an Ortec Model 9302 amplifier/discriminator and an RCA C31034 photomultiplier, and interfaced to an Intel 310 computer. The desired excitation wavelengths were provided by the following lasers: Spectra-Physics 2025-11 Kr, Coherent Innova 90-6 Ar, and Coherent 599-01 Dye (rhodamine 6G). Raman spectra were collected in an  $\sim 150^\circ$  backscattering geometry from samples maintained at  $\sim 15 \text{ K}$  using a closed-cycle helium refrigerator (Air Products Displex). Accurate peak heights and peak positions ( $\pm 1 \text{ cm}^{-1}$ ) were obtained by ordinate and abscissa expansion, respectively. For the enhancement profiles, all spectra were recorded on the same sample under the same instrumental conditions. Enhancement was measured as the height of the protein peak relative to the height of the ice peak at 230  $\text{cm}^{-1}$ , except for mutant SOD where peak areas were measured.

## Results and Discussion

**Resonance Raman Spectrum of Pseudoazurin.** Excitation of type 1 Cu proteins within the intense, 600-nm (Cys)S  $\rightarrow$  Cu(II) CT band leads to characteristic RR spectra having one to two vibrational fundamentals in the 250–280- $\text{cm}^{-1}$  region and as many as nine fundamentals in the 330–490- $\text{cm}^{-1}$  region.<sup>3</sup> Pseudoazurin from *A. faecalis* is a typical blue copper protein according to its X-ray crystal structure,<sup>24,25</sup> and it exhibits a typical type 1 Cu RR spectrum (Figure 1B).<sup>3</sup> In the 330–490- $\text{cm}^{-1}$  region, seven distinct peaks are observed at 340, 363, 385, 397, 415, 444, and 460  $\text{cm}^{-1}$ . The multiplicity of vibrational modes has been ascribed to kinematic coupling, an admixture of the Cu-S(Cys) stretch with cysteine and histidine ligand deformation modes.<sup>17,18</sup> Such coupling is favored by Cu-S <sub>$\gamma$</sub> -C <sub>$\beta$</sub> -C <sub>$\alpha$</sub>  and S <sub>$\gamma$</sub> -C <sub>$\beta$</sub> -C <sub>$\alpha$</sub> -N dihedral angles being close to 180°,<sup>17,26</sup> as is the case in pseudoazurin and a number of other type 1 Cu proteins.<sup>3</sup> The fact that these vibrational modes occur at a fairly constant set of frequencies in all blue copper proteins is a reflection of the highly conserved ground-state structure of the type 1 Cu site.<sup>3</sup>

In contrast, the RR spectra of different blue Cu proteins show a striking variability in vibrational peak intensities. For example, the strongest feature in the RR spectrum of pseudoazurin is at 397  $\text{cm}^{-1}$  (Figure 1B), whereas those for azurin and plastocyanin are at 408 and 425  $\text{cm}^{-1}$ , respectively.<sup>18</sup> Resonance Raman peak intensities are related to the change in geometry of the copper-cysteinyl chromophore in the electronic excited state. The intensity of a particular mode is maximized when the excited-state displacement of atoms occurs along the normal coordinate of the vibration.<sup>27,28</sup> It is likely that differences in protein structure beyond the first coordination sphere in different blue copper

(21) Hoitink, C. W. G.; Woudt, L. P.; Turenhout, J. C. M.; van de Kamp, M.; Canters, G. W. *Gene* **1990**, *90*, 15–20.

(22) Kakutani, T.; Watanabe, H.; Arima, K.; Beppu, T. *J. Biochem. (Tokyo)* **1981**, *89*, 463–472.

(23) Lu, Y.; LaCroix, L. B.; Lowery, M. D.; Solomon, E. I.; Bender, C. J.; Peisach, J.; Roe, J. A.; Gralla, E. G.; Valentine, J. S. *J. Am. Chem. Soc.*, in press.

(24) Petratos, K.; Dauter, Z.; Wilson, K. S. *Acta Crystallogr.* **1988**, *B44*, 628–636.

(25) Adman, E. T.; Turley, S.; Bramson, R.; Petratos, K.; Banner, D.; Tsernoglou, D.; Beppu, T.; Watanabe, H. *J. Biol. Chem.* **1989**, *264*, 87–99.

(26) Han, S.; Czernuszewicz, R. S.; Spiro, T. G. *J. Am. Chem. Soc.* **1989**, *111*, 3496–3504.

(27) Nishimura, Y.; Hirakawa, A. Y.; Tsuboi, M. In *Advances in Infrared and Raman Spectroscopy*; Clark, R. J. H., Hester, R. E., Eds.; Heyden: London, 1978; Vol. 5, pp 217–275.

(28) Shin, K.-S.; Zink, J. I. *Inorg. Chem.* **1989**, *28*, 4358–4366.

(15) Lu, Y.; Gralla, E. B.; Roe, J. A.; Valentine, J. S. *J. Am. Chem. Soc.* **1992**, *114*, 3560–3562.

(16) Lu, Y. Ph.D. Dissertation, University of California, Los Angeles, 1992.

(17) Nestor, L.; Larrabee, J. A.; Woolery, G.; Reinhammar, B.; Spiro, T. G. *Biochemistry* **1984**, *23*, 1084–1093.

(18) Blair, D. F.; Campbell, G. W.; Schoonover, J. R.; Chan, S. I.; Gray, H. B.; Malmström, B. G.; Pecht, I.; Swanson, B. I.; Woodruff, W. H.; Cho, W. K.; English, A. M.; Fry, H. A.; Lum, V.; Norton, K. A. *J. Am. Chem. Soc.* **1985**, *107*, 5755–5766.

(19) Ainscough, E. W.; Bingham, A. G.; Brodie, A. M.; Ellis, W. R.; Gray, H. B.; Loehr, T. M.; Plowman, J. E.; Norris, G. E.; Baker, E. N. *Biochemistry* **1987**, *26*, 71–82.

(20) Musci, G.; Desideri, A.; Morpurgo, L.; Tosi, L. *J. Inorg. Biochem.* **1985**, *23*, 93–102.

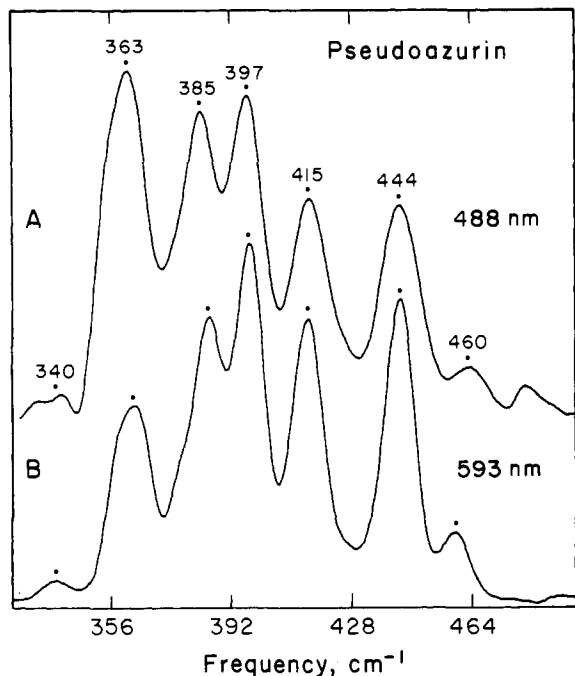


**Figure 1.** Resonance Raman spectra of pseudoazurin from *A. faecalis*. Spectra were obtained from 1.5 mM protein in 0.02 M phosphate, 0.04 M KCl (pH 6.3) using 488.0- and 593-nm excitation (60 mW) with a resolution of 5  $\text{cm}^{-1}$ , scan rate of 0.5  $\text{cm}^{-1}/\text{s}$ , and accumulation of 10 scans.

proteins affect the excited-state displacements, thereby explaining the variation in RR intensities.<sup>3</sup>

Excitation of pseudoazurin within its 450-nm absorption band (Figure 2) leads to the same set of RR frequencies (Figure 1A). There are, however, some alterations in RR intensities. For example, the peak at 363  $\text{cm}^{-1}$  has increased relative to the other modes. The constancy of frequencies shows that the electronic transitions at 450 and 590 nm arise from a common ground-state structure, i.e., a single type 1 Cu site. The variability in intensities, in this case, suggests that different electronic transitions are responsible for the 450- and 590-nm absorption bands.

**Resonance Raman Spectrum of Nitrite Reductase.** NiR from *A. cycloclastes* is a trimeric protein containing a type 1 Cu site (Figure 3, insert) in the amino-terminal domain of each monomer.<sup>9</sup> There is also a type 2 Cu site at a distance of 12.5 Å that is connected to the type 1 site by a His-Cys sequence where the His is coordinated to the type 2 Cu and the Cys is coordinated to the type 1 Cu. The type 2 site appears to be responsible for binding the nitrite substrate. NiR can be depleted of 80% of its type 2 Cu and lose 80% of its enzymatic activity, and still have an intact type 1 Cu site according to absorption and EPR spectroscopy.<sup>11</sup> The RR spectrum of type-2-depleted NiR (data not shown) is identical with that of the native enzyme (Figure 3A). This indicates the RR spectrum of NiR arises solely from the type 1 Cu site. Even though the type 1 Cys ligand is flanked by a His ligand to the type 2 site, there is no apparent change in the type 1 copper cysteine geometry upon removal of the type 2 copper.

The absorption spectrum of NiR is unusual for a type 1 site in that it exhibits four intense bands at 385, 460, 585, and 695 nm (Figure 4). Excitation within the predominant 460-nm absorption band produces the RR spectrum shown in Figure 3A. This spectrum is the same as that reported previously for *A. cycloclastes* NiR,<sup>12</sup> and it is characteristic of a type 1 Cu site. It exhibits one strong fundamental at 262  $\text{cm}^{-1}$  (a weaker peak at 280  $\text{cm}^{-1}$  tends to be obscured by the ice mode) and six distinct fundamentals at 343, 361, 395, 409, 424, and 443  $\text{cm}^{-1}$ . Excitation within the 585- and 695-nm absorption bands leads to a similar set of resonance-enhanced spectral features, unchanged in their vibrational energies (Figure 3, B and C). Thus, the same copper-

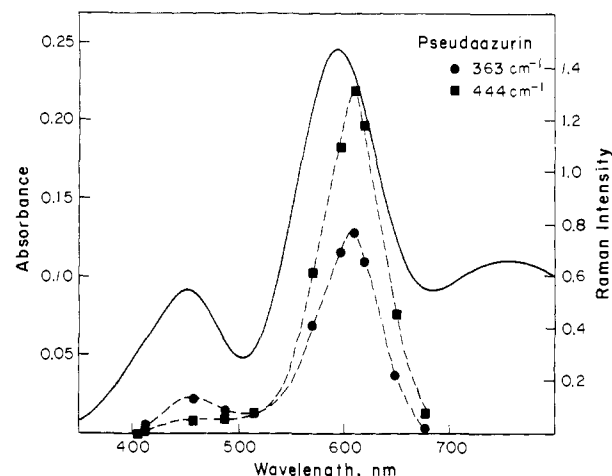


**Figure 2.** Absorption spectrum (—) and RR excitation profiles (---) for 363- and 444- $\text{cm}^{-1}$  modes of pseudoazurin. Raman data were obtained as in Figure 1, and peak heights were measured relative to the height of the 230- $\text{cm}^{-1}$  ice mode.

cysteinate moiety must be contributing to all three of these electronic transitions (Figure 4). A previous RR investigation of NiR also assigned the 460-nm absorption as S(Cys)  $\rightarrow$  Cu CT, but proposed that two separate Cu-S(Cys) moieties were responsible for the 460- and 585-nm transitions.<sup>12</sup> Those spectra, however, were obtained in glass capillaries and were distorted by the presence of an underlying glass band (between 350 and 520  $\text{cm}^{-1}$ ) in addition to low signal to noise. The present evidence for a *single Cu-S(Cys) chromophore* is compelling.

An interesting aspect of the RR spectrum of NiR is that the 361- $\text{cm}^{-1}$  peak is more enhanced with 477-nm excitation and actually becomes the dominant feature in the RR spectrum (Figure 3). This is similar to the behavior of pseudoazurin whose 363- $\text{cm}^{-1}$  peak is also the strongest spectral feature with 458- or 488-nm excitation (Figures 1 and 2). In a previous study, we noted that high Raman intensity in the 350–365- $\text{cm}^{-1}$  region appeared to correlate with the presence of a long loop of eight amino acids between the Cys 136 and His 145 ligands of NiR (Han et al., 1991). However, the present findings for pseudoazurin show that enhancement in the 350–365- $\text{cm}^{-1}$  region is also dependent on excitation wavelength. It cannot be just a function of loop size since pseudoazurin has only two amino acids in the loop connecting Cys 78 and His 81 ligands.<sup>24</sup>

**Resonance Raman Spectrum of Mutant Superoxide Dismutase.** In native yeast  $\text{Cu}_2\text{Zn}_2\text{SOD}$ ,<sup>14</sup> the Zn(II) in each subunit is ligated to His 71, His 80, and Asp 83, with the imidazole of His 63 bridging the Zn and Cu ions (Scheme I). The Zn(II) site has a geometry close to tetrahedral. When the His 80 ligand is converted to Cys by site-directed mutagenesis and the protein is reconstituted with four Cu(II), the resultant protein has the EPR properties of a 1:1 mixture of type 1 and type 2 copper sites.<sup>15,23</sup> The type 1 component, arising from the original zinc site, is responsible for the green color of the mutant protein and yields a RR spectrum typical of a blue copper protein (Figure 5). Two vibrational fundamentals appear at 259 and 280  $\text{cm}^{-1}$ , and six higher-energy fundamentals are seen at 341, 352, 398, 415, 435, and 468  $\text{cm}^{-1}$ . In addition, a number of less intense bands are observed at even higher energy at 606, 702, 754, and 813  $\text{cm}^{-1}$  (Figure 5, insert) that are also characteristic of type 1 Cu sites.<sup>18</sup> These bands can be ascribed, respectively, to a combination band (352 + 259 = 611), an overtone ( $2 \times 352 = 704$ ), the C-S stretch of cysteine at 754  $\text{cm}^{-1}$ , and another combination band (352 + 468 = 820).

The RR spectrum of H80C-Cu<sub>2</sub>Cu<sub>2</sub>SOD is clearly indicative of copper cysteine coordination. The similarity of vibrational frequencies to other type 1 copper sites suggests a number of common structural features. (i) The multiple vibrational modes

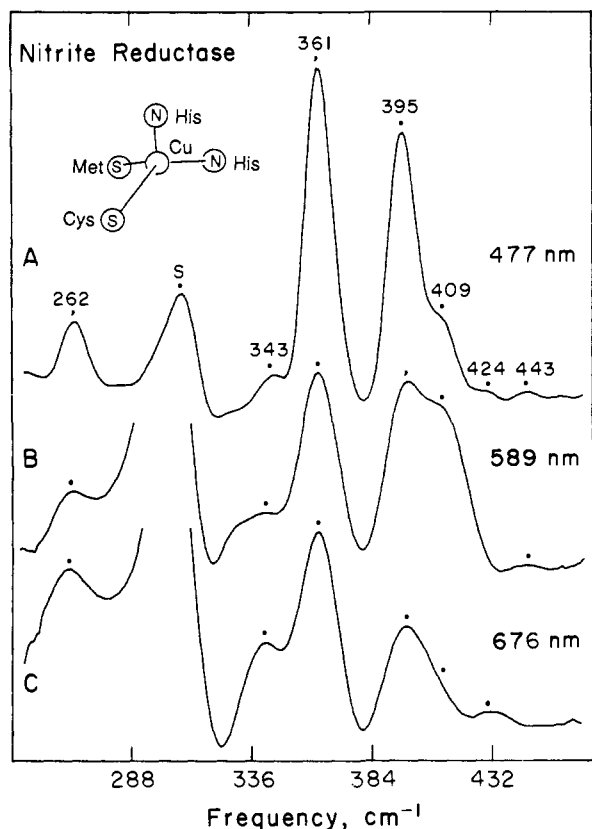


**Figure 3.** Resonance Raman spectra of nitrite reductase from *A. cycloclastes*. Spectra were obtained from protein 0.59 mM in type 1 Cu in 0.05 M MES (pH 6.4) in D<sub>2</sub>O using 476.5-, 589-, and 676.4-nm excitation ( $\sim 120$  mW) with a resolution of  $8\text{ cm}^{-1}$ , scan rate of  $1\text{ cm}^{-1}/\text{s}$ , and accumulation of 15 scans. S denotes peak from frozen solvent and is set offscale in the lower two spectra. The insert shows the coordination of the type 1 Cu site (Godden et al., 1991).

arise from coupling of the Cu–S(Cys) stretch with Cys and other ligand deformations. (ii) The conserved nature of the Cu–S stretching and Cys bending force constants requires a similarly short Cu–S(Cys) bond length of  $\sim 2.12 \pm 0.05\text{ \AA}$ .<sup>3</sup> (iii) The kinematic coupling further requires a coplanar orientation for the Cys 80 ligand with a Cu–S <sub>$\gamma$</sub> –C <sub>$\beta$</sub> –C <sub>$\alpha$</sub>  dihedral angle close to  $180^\circ$ . (iv) The short Cu–S(Cys) bond implies a trigonal-planar array of ligands.<sup>29</sup>

The electronic and RR spectral properties of the type 1 Cu site in H80C–Cu<sub>2</sub>Zn<sub>2</sub>SOD appear closely related to those of the type 1 Cu site in NiR. The absorption spectrum exhibits two strong components at 458 and 597 nm, with the 458-nm band being slightly more intense (Figure 6). Excitation within either absorption band yields the same RR spectrum (Figure 5), suggesting that both absorptions involve S(Cys)  $\rightarrow$  Cu(II) CT transitions. The extent of resonance enhancement (as judged by the intensity of the protein Raman peaks relative to the ice mode) is comparable to other type 1 Cu proteins (Figures 2, 4, and 6), indicating similar displacements in the electronic excited state. The only differences in the RR spectra of mutant SOD between 647- and 458-nm excitation are increased intensities at 296 and 341  $\text{cm}^{-1}$  and decreased intensities at 259 and 280  $\text{cm}^{-1}$  (Figure 5). An unusual aspect relative to other blue copper proteins is that the RR spectrum of mutant SOD is so strongly dominated by the peak at 352  $\text{cm}^{-1}$  at all excitation wavelengths, with only weakly enhanced bands in the 380–480- $\text{cm}^{-1}$  region. The RR spectra of NiR also lack intensity in the 420–480- $\text{cm}^{-1}$  region, but the effect is considerably more pronounced for mutant SOD.

(29) (a) Kitajima, N. *Adv. Inorg. Chem.*, in press. (b) Kitajima, N.; Fujisawa, K.; Tanaka, M.; Moro-oka, Y. *J. Am. Chem. Soc.* **1992**, *114*, 9232–9233.

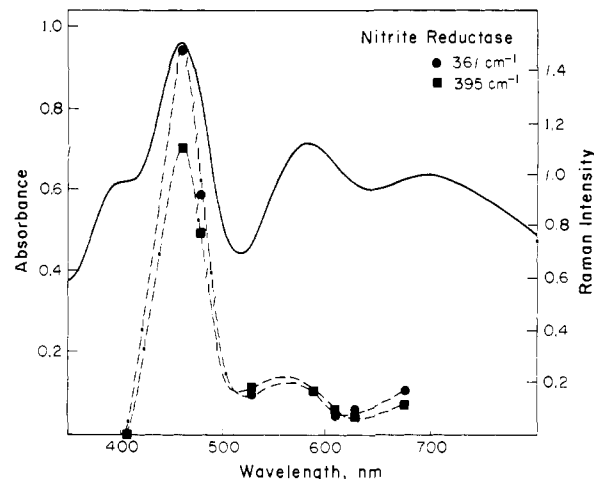


**Figure 4.** Absorption spectrum (—) and RR excitation profiles (---) for 361- and 395- $\text{cm}^{-1}$  modes of nitrite reductase. Raman data were obtained as in Figure 3, and peak heights were measured relative to the height of the 230- $\text{cm}^{-1}$  ice mode.

Two additional mutants of yeast SOD, each with a cysteine in place of a Cu-site histidine (Scheme I), were examined. These were H46C–Cu<sub>2</sub>Zn<sub>2</sub>SOD<sup>15</sup> and H120C–Cu<sub>2</sub>Zn<sub>2</sub>SOD.<sup>16</sup> Cysteinate coordination of the copper in each mutant is evident from the appearance of a S(Cys)  $\rightarrow$  Cu(II) CT band at 379 nm ( $\epsilon = 1940\text{ M}^{-1}\text{ cm}^{-1}$ ) and 406 nm ( $\epsilon = 1120\text{ M}^{-1}\text{ cm}^{-1}$ ), respectively. The high energy of these electronic transitions is suggestive of tetragonal rather than tetrahedral coordination geometry.<sup>30a</sup> For example, tetragonal cupric thiolate complexes often exhibit absorption maxima at 400–430  $\text{cm}^{-1}$  with  $\epsilon = 1000\text{--}6500\text{ M}^{-1}\text{ cm}^{-1}$ .<sup>29</sup> Excitation of the H46C mutant at 350.8 nm produced a weak RR spectrum with the most distinct peak at 343  $\text{cm}^{-1}$ ; excitation of the H120C mutant at 406.7 nm yielded an even weaker RR spectrum with a detectable peak at 367  $\text{cm}^{-1}$  (data not shown).<sup>30b</sup> The weak resonance enhancement and large EPR  $A_{\parallel}$  values (Table I) are also consistent with a tetragonal coordination assignment.

**Raman Intensities for Type 1 versus Type 2 Copper.** The major criterion for distinguishing between type 1 and type 2 copper has been the EPR hyperfine splitting, with small  $A_{\parallel}$  values of  $30\text{--}70 \times 10^{-4}\text{ cm}^{-1}$  defining a type 1 site and larger  $A_{\parallel}$  values of  $130\text{--}180 \times 10^{-4}\text{ cm}^{-1}$  defining a type 2 site (Table I). Crystal structures of proteins and model compounds have revealed that, whereas type 2 Cu tends to have four strongly coordinated ligands in a tetragonal array and a Cu–S bond distance  $\geq 2.25\text{ \AA}$ , type 1 Cu tends to be associated with a trigonal-planar ligand set. This decrease in the number of strongly coordinated ligands is presumably responsible for the shortening of the Cu–S bond to  $\sim 2.15\text{ \AA}$  (Table I) and the change in the EPR hyperfine character.

(30) (a) Lever, A. B. P. In *Inorganic Electronic Spectroscopy*; Elsevier: Amsterdam, 1984; pp 303–308. (b) Andrew, C. R.; Yeom, H.; Valentine, J. S.; Sanders-Loehr, J. Unpublished results.

(31) Sharma, K. D.; Loehr, T. M.; Sanders-Loehr, J.; Husain, M.; Davidson, V. L. *J. Biol. Chem.* **1988**, *263*, 3303–3306.

(32) Maret, W.; Shiemke, A. K.; Wheeler, W. D.; Loehr, T. M.; Sanders-Loehr, J. *J. Am. Chem. Soc.* **1986**, *108*, 6351–6359.

(33) Maret, W.; Kozlowski, H. *Biochim. Biophys. Acta* **1987**, *912*, 329–337.

(34) Brader, M. L.; Borchardt, D.; Dunn, M. F. *J. Am. Chem. Soc.* **1992**, *114*, 4480–4486.

(35) Spiro, T. G. Personal communication.

(36) Thompson, J. S.; Marks, T. J.; Ibers, J. A. *J. Am. Chem. Soc.* **1979**, *101*, 4180–4192.

(37) Anderson, O. P.; Becher, J.; Frydendahn, H.; Taylor, L. F.; Toftlund, H. *J. Chem. Soc., Chem. Commun.* **1986**, 699–701.

(38) Jensen, R. W.; Becher, J.; Toftlund, H. In *Spectroscopy of Biological Molecules*; Alix, A. J. P., Bernard, L., Manfait, M., Eds.; John Wiley: New York, 1985; pp 205–207.

(39) Sharma, K. D.; Sanders-Loehr, J.; Toftlund, H. Unpublished results.

(40) Taylor, M. R.; Glusker, J. P.; Gabe, E. J.; Minkin, J. A. *Bioinorg. Chem.* **1974**, *3*, 189–205.

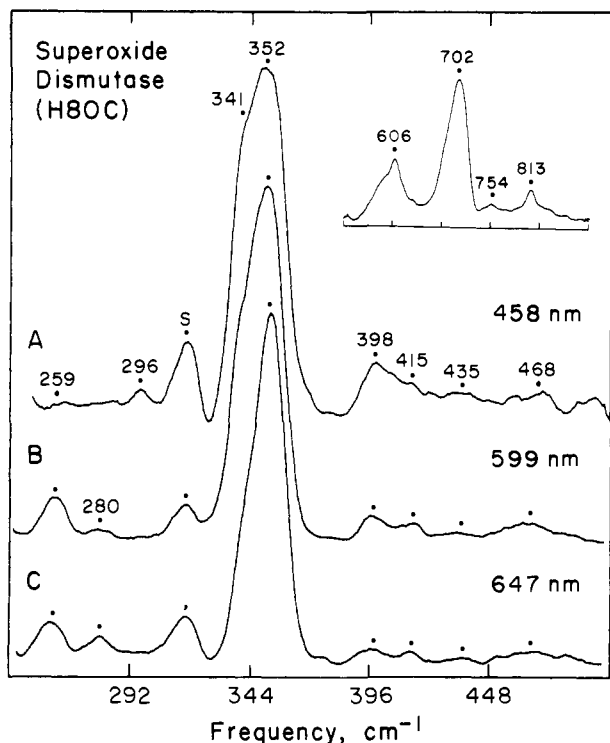


**Figure 5.** Resonance Raman spectra of mutant superoxide dismutase (H80C-Cu<sub>2</sub>Cu<sub>2</sub>) from *S. cerevisiae*. Spectra were obtained from 0.75 mM protein (1.5 mM in type 1 Cu) in 0.1 M acetate (pH 5.5) using 457.9-, 599-, and 647.1-nm excitation (~65 mW) with a resolution of 7.5 cm<sup>-1</sup>, scan rate of 0.5 cm<sup>-1</sup>/s, and accumulation of 4, 4, and 16 scans, respectively. The insert shows the overtone region of the same sample obtained as above with 610-nm excitation (80 mW) and 17 scans.

For type 2 Cu, the wavelength of the most intense thiolate → Cu(II) CT band is quite variable, with absorption maxima ranging from 380 to 590 nm (Table I). This electronic transition is somewhat less variable for type 1 Cu with maximum absorption occurring either at 595–665 nm or near 460 nm. Despite the variability in absorption maxima, it appears that type 1 and type 2 Cu sites can be distinguished by their different extents of RR intensity enhancement.

For solids or samples in aqueous solution, Raman intensities can be quantitated relative to the intensity of the 980-cm<sup>-1</sup> symmetric stretch of a sulfate internal standard. The type 1 copper proteins (1–6) listed in Table I have large Raman enhancements with molar scattering intensities of 100–600 relative to sulfate. The molar scattering values ≥ 500 tend to be associated with  $\epsilon$  values near 5000 M<sup>-1</sup> cm<sup>-1</sup>, whereas those in the 100–200 range are associated with  $\epsilon$  values near 2500 M<sup>-1</sup> cm<sup>-1</sup>. This is commensurate with the expectation that Raman intensities for symmetric vibrations are proportional to  $\epsilon^2$ .<sup>18</sup> The sterically hindered Cu complexes (8, 9) with tris(pyrazolyl)borate and SCPh<sub>3</sub> or SC<sub>6</sub>F<sub>5</sub> as ligands are the first small-molecule models

(41) Tosi, L.; Garnier-Suillerot, A. *J. Chem. Soc. Dalton Trans.* **1982**, 103–108.

(42) Hughey, J. L., IV; Fawcett, T. G.; Rudich, S. M.; Lalancette, R. A.; Potenza, J. A.; Schugar, H. J. *J. Am. Chem. Soc.* **1979**, *101*, 2617–2623.

(43) Birker, P. J. M. W. L.; Freeman, H. C. *J. Am. Chem. Soc.* **1977**, *99*, 6890–6899.

(44) Tosi, L.; Garnier, A. *Biochem. Biophys. Res. Commun.* **1979**, *91*, 1273–1279.

(45) Bharadwaj, P. K.; Potenza, J. A.; Schugar, H. J. *J. Am. Chem. Soc.* **1986**, *108*, 1351–1352.

(46) den Blaauwen, T.; van de Kamp, M.; Canters, G. W. *J. Am. Chem. Soc.* **1991**, *113*, 5050–5052.

(47) den Blaauwen, T.; Canters, G. W. *J. Am. Chem. Soc.* **1992**, *115*, 1121–1129.

(48) (a) Han, J.; Loehr, T. M.; Sanders-Loehr, J.; den Blaauwen, T.; Canters, G. W. Unpublished results. (b) Sanders-Loehr, J. In *Bioinorganic Chemistry of Copper*; Karlin, K. D., Tyeklar, Z., Eds.; Chapman & Hall: New York, 1993; pp 51–63.

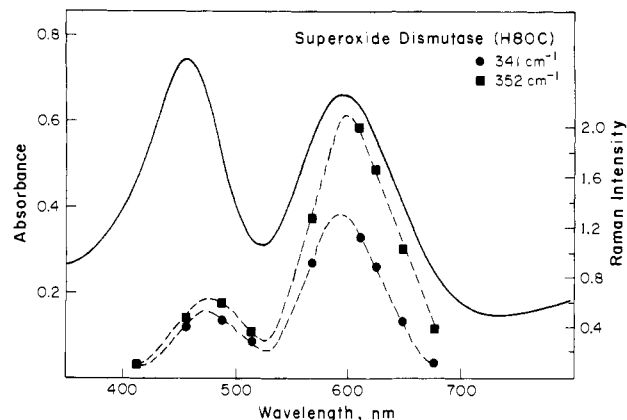


**Figure 6.** Absorption spectrum (—) and RR excitation profiles (---) for 341- and 352-cm<sup>-1</sup> modes of mutant superoxide dismutase. Raman data were obtained as in Figure 5, and peak areas were measured relative to the area of the 230-cm<sup>-1</sup> ice mode using a planimeter. The overlapping peaks at 341 and 352 cm<sup>-1</sup> were resolved by curve-fitting (Galactic LabCalc).

**Table I.** Properties of Cupric Thiolate Complexes

compound <sup>a</sup>	Cu-S distance, Å	EPR <sup>b</sup> A <sub>1</sub>	S → Cu CT <sup>c</sup>		Raman intensity <sup>d</sup>
			$\lambda_{\max}$	$\epsilon$	
Type 1 Cu Sites					
1 amicyanin		50	595	4610	500
2 azurin	2.13	60	619	5100	~650
3 pseudoazurin	2.16	55	593	2900	~130
4 nitrite reductase	2.15	69	458	2530	~200
5 SOD-Cu <sub>2</sub> Cu <sub>2</sub> (H80C)	15	595	>1420		~150
6 LADH-Cu	50	623	2450		~120
7 Cu <sub>2</sub> (insulin) <sub>6</sub> (SC <sub>6</sub> F <sub>5</sub> ) <sub>2</sub>		27	630	1800	<i>e</i>
8 Cu(Pz) <sub>3</sub> (SCPh <sub>3</sub> )	2.12	74	625	6600	<i>e</i>
9 Cu(Pz) <sub>3</sub> (SC <sub>6</sub> F <sub>5</sub> )	2.18	54	665	5960	<i>e</i>
Type 2 Cu Sites					
10 Cu(Pz) <sub>3</sub> (SC <sub>6</sub> H <sub>4</sub> NO <sub>2</sub> )	171	588	3900		<i>e</i>
11 Cu(diimino)-(S-pyrazole) <sub>2</sub>	2.25	137	535	3000	20
12 Cu(thiosemicarbazone) <sub>2</sub>	2.26		469	6300	60
13 Cu(tetraazo)-(SC <sub>6</sub> H <sub>4</sub> CO <sub>2</sub> ) <sub>2</sub>	2.36		418	1100	
14 Cu(N <sub>2</sub> S <sub>2</sub> -penicillamine)	2.28		518	4250	<i>e</i>
15 Cu(diamino)-(SCH <sub>2</sub> CH) <sub>2</sub>	2.25	182	400	>1000	10
16 SOD-Cu <sub>2</sub> Zn <sub>2</sub> (H46C)		151	379	1940	~20
17 SOD-Cu <sub>2</sub> Zn <sub>2</sub> (H120C)		175	406	1250	~15
18 azurin(H117G) + His		156	400	~2800	~50
19 LADH-Cu + imidazole		127	480	~2000	~20

<sup>a</sup> Compounds and data from following sources: 1, *Paracoccus denitrificans* (ref 31); 2, *A. denitrificans* (ref 19), Raman spectrum of *P. aeruginosa*; 3, *A. faecalis* S-6 (ref 22, 24); 4, *A. cycloclastes* (refs 11, 59); 5, *S. cerevisiae* (refs 16, this work); 6, Cu-substituted liver alcohol dehydrogenase (refs 32, 33); 7, insulin complexed to Cu and benzenethiolate (ref 34); 8, 9, Cu[HB(3,5-*i*Pr<sub>2</sub>pz)<sub>3</sub>](L) where L = SCPh<sub>3</sub> or SC<sub>6</sub>F<sub>5</sub> (ref 29), Raman spectrum (ref 35); 10, Cu[HB(3,5-Me<sub>2</sub>pz)<sub>3</sub>](SC<sub>6</sub>H<sub>4</sub>NO<sub>2</sub>) (ref 36); 11, Cu[2,2'-bis(1-phenyl-3-methyl-5-thiopyrazol-4-ylmethyl-eneamino)biphenyl] (ref 37), Raman spectrum (refs 38, 39); 12, Cu[3-ethoxy-2-oxobutylaldehyde bis(thiosemicarbazone)] (ref 40), Raman spectrum (ref 41); 13, Cu complex with a tetraazocyclotetradecane and (*o*-SC<sub>6</sub>H<sub>4</sub>CO<sub>2</sub>)<sup>-</sup> (ref 42); 14, [(Cu<sup>II</sup>)<sub>6</sub>(Cu<sup>I</sup>)<sub>8</sub>(*o*-penicillamine)<sub>2</sub>Cl]<sup>3-</sup> (refs 43, 44); 15, Cu[SCH<sub>2</sub>CH(CO<sub>2</sub>CH<sub>3</sub>)NHCH<sub>2</sub>]<sub>2</sub> (ref 45), Raman on Cu[SC(CH<sub>3</sub>)<sub>2</sub>CH<sub>2</sub>NHCH<sub>2</sub>]<sub>2</sub> (ref 39); 16, 17, *S. cerevisiae* (refs 16, 30b); 18, *P. aeruginosa* azurin mutant (H117G) plus exogenous histidine (refs 46–48); 19, Cu-substituted LADH plus exogenous imidazole (ref 32). <sup>b</sup> A<sub>1</sub> in cm<sup>-1</sup> × 10<sup>-4</sup>. <sup>c</sup>  $\lambda_{\max}$  in nm,  $\epsilon$  in M<sup>-1</sup> cm<sup>-1</sup> per Cu. <sup>d</sup> Intensity of strongest RR peak relative to intensity of 980-cm<sup>-1</sup> peak of sulfate (accuracy ±20%). Data obtained with excitation close to  $\lambda_{\max}$  and calculated per mole of Raman scatterer. Approximate intensity (~) obtained relative to 230-cm<sup>-1</sup> ice mode and normalized to value for sulfate, based on liquid and frozen solution data for amicyanin (accuracy ±30%). <sup>e</sup> RR spectrum observed, but molar scattering intensity not quantitated.

in which type 1 Cu properties have been duplicated. Each of these complexes has a CuN<sub>2</sub>S cluster in a trigonal-planar array

with an unusually short Cu-S bond and narrow hyperfine splitting.<sup>29</sup> These complexes also yield a set of strongly enhanced Raman modes derived from the Cu-SR moiety.<sup>35</sup>

Although the type 2 copper complexes (10–15) and proteins (16–19) in Table I exhibit extinction coefficients of similar magnitude to the type 1 complexes (i.e., 1000–6000 M<sup>-1</sup> cm<sup>-1</sup>), they give rise to considerably less RR enhancement of Cu-thiolate vibrational modes. The observed molar scattering values of 10–60 relative to sulfate are 5–10 times smaller than for the corresponding type 1 sites with similar extinction coefficients. Thus, it would appear that the Cu-cysteinate moiety in type 1 Cu undergoes a greater change in geometry in the excited state, leading to more extensive vibronic coupling than is observed for type 2 Cu.

**Raman Excitation Profiles.** An excitation profile for a particular vibrational mode is obtained by collecting RR spectra at a number of different excitation wavelengths and plotting the vibrational intensity as a function of wavelength. Peaks in the excitation profile are expected to correspond with peaks in the electronic spectrum. If the atoms responsible for the vibrational mode are known, this information can be used to assign the nature of the electronic transition. A typical RR excitation profile for a blue copper protein is shown in Figure 7 for azurin from *A. denitrificans*. All of the vibrational features have maximum intensity corresponding to the 619-nm absorption band. Similar findings have been reported previously for this azurin<sup>19</sup> and for stellacyanin.<sup>20</sup> These results show that all of the vibrational modes are associated with the same chromophoric species. Isotope and ligand-substitution experiments,<sup>17,18,49</sup> as well as MCD and single-crystal polarized absorption experiments,<sup>5,6</sup> all point to the Cu-cysteinate moiety as the chromophore responsible for the ~600-nm absorption and, thus, many of the observed RR modes.

Although a strong absorption band near 600 nm has been the hallmark for type 1 Cu, there is a 2.5-fold variability in the magnitude of the extinction coefficient (Table II). There appears to be a corresponding, but inverse, variability in the magnitude of the absorption band near 460 nm, such that  $\epsilon_{460}$  increases as  $\epsilon_{600}$  decreases. The ratio of the 460- and 600-nm absorption intensities ( $R_{abs}$ ) ranges from 0.11 for azurin to 1.34 for NiR (Table II). However, the sum of  $\epsilon_{460} + \epsilon_{600}$  is remarkably constant at 4000–5000 M<sup>-1</sup> cm<sup>-1</sup>. This interrelationship between the two absorption bands is further supported by our RR data. The Raman spectra for pseudoazurin (Figure 1), nitrite reductase (Figure 3), mutant SOD (Figure 5), and azurin show that *the same vibrational modes are observed upon excitation within either absorption band*. Furthermore, in the excitation profiles for pseudoazurin (Figure 2), nitrite reductase (Figure 4), mutant SOD (Figure 6), and azurin (Figure 7), the intensity of each RR peak tracks both the 460- and 600-nm absorption bands. Given the dominant contribution of the cysteine ligand to the 600-nm absorption and concomitant RR spectrum, it is likely that the 460-nm electronic transition has substantial Cu-cysteinate character, as well.

The excitation profiles also show that the relative intensities of the different RR peaks do vary as a function of excitation

(49) Thamann, T. J.; Frank, P.; Willis, L. J.; Loehr, T. M. *Proc. Natl. Acad. Sci. U.S.A.* **1982**, *79*, 6396–6400.

(50) Katoh, S.; Shiratori, I.; Takamiya, A. *J. Biochem. (Tokyo)* **1962**, *51*, 32.

(51) Guss, J. M.; Bartunik, H. D.; Freeman, H. C. *Acta Cryst. B* **1992**, *48*, 790–811.

(52) Baker, E. N. *J. Mol. Biol.* **1988**, *203*, 1071–1095.

(53) Husain, M.; Davidson, V. L. *J. Biol. Chem.* **1985**, *260*, 14626–14629.

(54) Romero, A.; Hoihtink, C. W. G.; Nar, H.; Huber, R.; Messerschmidt, A.; Canters, G. W. *J. Mol. Biol.*, in press.

(55) McManus, J. D.; Brune, D. C.; Han, J.; Sanders-Loehr, J.; Meyer, T. E.; Cusanovich, M. A.; Tollin, G.; Blankenship, R. E. *J. Biol. Chem.* **1992**, *267*, 6531–6540.

(56) Sakurai, T.; Sawada, S.; Nakahara, A. *Inorg. Chim. Acta* **1986**, *123*, L21–L22.

(57) Guss, J. M.; Freeman, H. C. Personal communication.

(58) Blake, R. C., II; Shute, E. A. *J. Biol. Chem.* **1987**, *262*, 14983–14989.

(59) Adman, E. T. Personal communication.

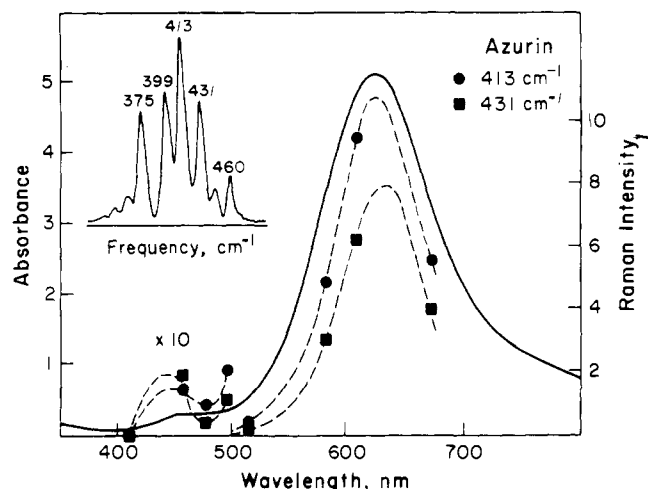


Figure 7. Absorption spectrum (—) and RR excitation profiles (---) for 413- and 431-cm<sup>-1</sup> modes of azurin from *A. denitrificans*. The Raman spectrum in the insert was obtained on 2 mM protein in 0.02 M Tris-Cl (pH 8.4) using 609-nm excitation (60 mW), a resolution of 5 cm<sup>-1</sup>, scan rate of 0.5 cm<sup>-1</sup>/s, and accumulation of 8 scans. Raman spectra at other excitation wavelengths were similarly collected, and peak heights were measured relative to the height of the 230-cm<sup>-1</sup> ice mode. The enhancement in the 400–500-nm region has been multiplied by a factor of 10.

wavelength. For example, with 460-nm excitation of pseudoazurin, the 363-cm<sup>-1</sup> peak exhibits increased intensity relative to the 444-cm<sup>-1</sup> peak (Figures 1 and 2). Similar relative intensity increases with 460-nm excitation are observed for the 361- versus 395-cm<sup>-1</sup> peak in nitrite reductase (Figure 4), the 341- versus 352-cm<sup>-1</sup> peak in mutant SOD (Figure 6), and the 431- versus 413-cm<sup>-1</sup> peak in azurin (Figure 7). Since RR intensities are determined by changes in the nuclear coordinates of bonded atoms between the ground state and the excited state,<sup>27</sup> the variability in RR intensities indicates that the ~460-nm absorption band arises from a different electronic transition. The constancy of vibrational frequencies suggests a common copper-cysteinate ground state that leads to a somewhat different set of excited-state structures upon absorption of 460- or 600-nm radiation.

**Assignment of Electronic Transitions in Type 1 Cu Sites.** Previous analyses of type 1 Cu proteins, particularly by CD and MCD spectroscopy, have revealed the presence of at least three electronic transitions between 400 and 550 nm.<sup>5,6</sup> For plastocyanin these have been specifically assigned to Met → Cu(II) CT at 430 nm, His → Cu(II) CT at 465 nm, and Cys → Cu(II) CT at 535 nm. Other type 1 proteins such as pseudoazurin, nitrite reductase, and mutant SOD show markedly increased absorption intensities in this region (Figures 2, 4, and 6), leading to the question of whether the plastocyanin assignments are generally applicable to all type 1 copper sites.

The methionine assignment is problematical because excitation within the 430-nm region does not lead to the appearance of any new RR features that could be associated with vibrations of a methionine ligand. Furthermore, replacement of the methionine ligand in *P. aeruginosa* (*P.a.*) azurin by selenomethionine causes no perturbation in the 430-nm spectral region<sup>60</sup> and no change in the RR spectrum.<sup>49</sup> Replacement of the Met 121 ligand in *A. denitrificans* azurin by a ligating glutamine results in *increased* rather than decreased intensity at 430–460 nm.<sup>54</sup> Removal of the Met 121 ligand in *P.a.* azurin by cleavage of the polypeptide chain after residue 120 also results in a more prominent absorption band at 450 nm.<sup>61</sup> Thus, additional electronic transitions unrelated to methionine are clearly present in this spectral region.

(60) Frank, P.; Licht, A.; Tullius, T. D.; Hodgson, K. O.; Pecht, I. *J. Biol. Chem.* **1985**, *260*, 5518–5525.

(61) Karlsson, B. G.; Nordling, M.; Pascher, T.; Tsai, L.-C.; Sjölin, L.; Lundberg, L. G. *Protein Eng.* **1991**, *4*, 343–349.

Table II. Properties of Type 1 Copper Sites

EPR spectrum <sup>a</sup>	absorption band near 460 nm <sup>b</sup>		absorption band near 600 nm <sup>b</sup>		$R_{\text{abs}}$ ( $\epsilon_{460}/\epsilon_{600}$ )	Cu-X (axial) distance, Å <sup>c</sup>	Cu <sup>III</sup> (NNS) distance, Å <sup>d</sup>
	$\lambda_{\text{max}}$	$\epsilon$	$\lambda_{\text{max}}$	$\epsilon$			
axial							
Cu(Pz <sub>3</sub> )(SCPh <sub>3</sub> ), 8 <sup>e</sup>	440	340	625	6600	0.05	2.03 (N)	0.20
Cu(Pz <sub>3</sub> )(SC <sub>6</sub> F <sub>5</sub> ), 9 <sup>e</sup>	420	630	665	5960	0.11	2.04 (N)	0.34
plastocyanin <sup>f</sup>	460	590	597	4900	0.12	2.82 (S)	0.36
azurin <sup>g</sup>	460	580	619	5100	0.11	3.13 (S)	0.12
amicyanin <sup>h</sup>	464	520	595	4610	0.11		
rhombic							
azurin(M121Q) <sup>i</sup>	452	1200	610	6000	0.20	2.27 (O)	0.26
stellacyanin <sup>j</sup>	450	1100	608	4080	0.27		
auracyanin A <sup>k</sup>	454	900	596	3000	0.30		
pseudoazurin <sup>l</sup>	450	1180	593	2900	0.41	2.76 (S)	0.43
cucumber basic protein <sup>m</sup>	448	1240	593	2900	0.43	2.62 (S)	0.39
rusticyanin <sup>n</sup>	445	1000	600	2100	0.47		
SOD-Cu <sub>2</sub> Cu <sub>2</sub> (H80C) <sup>o</sup>	459	>1460	595	>1420	1.03		
nitrite reductase <sup>p</sup>	458	2530	585	1890	1.34	2.62 (S)	0.50

<sup>a</sup> Axial versus rhombic character of X-band EPR spectra described in ref 23. <sup>b</sup>  $\lambda_{\text{max}}$  in nm,  $\epsilon$  in  $\text{M}^{-1} \text{cm}^{-1}$  per type 1 Cu. <sup>c</sup> Distance to axial ligand, X = N(Pz), S(Met), or O(Gln). <sup>d</sup> Distance of Cu from plane of three ligands; N = His, S = Cys in proteins. <sup>e</sup> Cu[HB(3,5-*i*Pr<sub>2</sub>pz)<sub>3</sub>](L) (ref 29)/ Spinach, optical and EPR (ref 50); *P. nigra* X-ray structure at 1.33-Å resolution (ref 51). <sup>f</sup> *A. denitrificans* (refs 19, 52). <sup>g</sup> *P. denitrificans* (ref 53). <sup>h</sup> *A. faecalis* S-6 mutant (ref 54). <sup>i</sup> *Rhus vernicifera* (ref 20). <sup>j</sup> *Chloroflexus aurantiacus* (ref 55). <sup>k</sup> *A. faecalis* S-6 (refs 22, 24). <sup>l</sup> (refs 56, 57). <sup>m</sup> *Thiobacillus ferrooxidans* (ref 58). <sup>n</sup> *S. cerevisiae* (ref 16). <sup>o</sup> *A. cycloclastes* (refs 11, 59).

The His → Cu(II) CT assignment at 460 nm is supported by single-crystal studies of plastocyanin which indicate that this absorption band is more polarized in the direction of the two histidine ligands than is the 600-nm absorption band.<sup>5b</sup> New information has been obtained using histidine ligand mutants of *P. a. azurin*. (i) Reconstitution of the His117Gly mutant with exogenous imidazole yields a species almost identical with wild-type in its absorption spectrum,<sup>46,47</sup> RR frequencies (all within 2  $\text{cm}^{-1}$ ), RR molar scattering intensity ( $\sim 600$ ), and relative RR intensities.<sup>48</sup> (ii) Reconstitution of the His117Gly mutant with [<sup>15</sup>N]-imidazole does not cause any detectable isotope shifts in the 350–500- $\text{cm}^{-1}$  region. (iii) Replacement of either the His 117 ligand by chloride<sup>47,48</sup> or the His 46 ligand by aspartate,<sup>62</sup> causes no decrease in the intensity of the 460-nm absorption band and produces very little change in the RR spectrum. For example, in the RR spectrum of the H117G mutant plus chloride, most of the frequencies are within 2–4  $\text{cm}^{-1}$  of wild-type azurin and only 3 of the 11 peaks have changed in intensity. Since the RR spectrum of azurin appears to be dominated by the Cu–cysteinate moiety, it is likely that both the 460- and 600-nm absorption bands have substantial S(Cys) → Cu(II) CT contributions.

The alternative that a His → Cu(II) CT transition at 460 nm adds electron density into cysteine orbitals remains a possible explanation for the RR results. However, the Raman intensity patterns obtained via 460- and 600-nm excitation are strikingly similar. This would require that electron density derived from either a Cys or a His ligand could produce a similar structural change in going from the ground state to the excited state. Furthermore, the large molar absorptivities at 460 nm ( $\epsilon > 1000 \text{ M}^{-1} \text{cm}^{-1}$ ) for many type 1 copper proteins (Table II) seem more compatible with a Cys → Cu(II) CT assignment. Cupric thiolate complexes typically yield  $\epsilon$  values of this magnitude (Table I). In contrast, cupric imidazole complexes tend to have weaker absorption bands in this region. For example, the Cu(II) complex with the constrained bidentate ligand, 2,2'-bis(2-imidazolyl)-biphenyl, has an imidazole → Cu CT band at 440 nm but its  $\epsilon$  value is only 260  $\text{M}^{-1} \text{cm}^{-1}$ .<sup>63</sup> In addition, cupric imidazole complexes are very weak Raman scatterers.<sup>64</sup> Yet the RR spectrum of nitrite reductase obtained with 460-nm excitation is

as strongly enhanced (molar scattering  $\approx 200$ ) as the RR spectra of other type 1 sites obtained with 600-nm excitation (Table I). These results imply that Cys → Cu CT is a major contributor to the 460-nm absorption band in many type 1 copper proteins.

The assignment of a second Cys → Cu CT transition at 460 nm suggests an explanation for the variability and approximate additivity of the  $\epsilon$  values for the 460- and 600-nm absorption bands (Table II). The actual absorption intensity associated with each band would be expected to depend on the relative alignment of the sulfur p orbitals with respect to the Cu d orbitals for each type 1 Cu site. Perturbations in these alignments would alter the degree of orbital overlap and, thus, alter the relative transition probabilities in different type 1 copper proteins.

**Correlation of Electronic, EPR, and Structural Properties.** The EPR definition of a type 1 Cu species is the appearance of narrow hyperfine splitting in the  $A_{\parallel}$  region (Table I). This can be ascribed to the influence of a short Cu–S(Cys) bond in a trigonal-pyramidal structure. However, within this category there is surprising variability in the rhombicity of the EPR spectrum, ranging from strongly axial as in plastocyanin to strongly rhombic as in stellacyanin.<sup>4</sup> The rhombic distortion should be reflecting a further loss of symmetry in the type 1 site. A correlation between the occurrence of a rhombic EPR signal and the appearance of the 460-nm absorption band has been noted by Lu et al.<sup>23</sup> As indicated in Table II, type 1 sites with a weak 460-nm band ( $\epsilon < 600 \text{ M}^{-1} \text{cm}^{-1}$ ) and an  $R_{\text{abs}} \leq 0.12$  have axial EPR spectra. Type 1 sites with a more intense 460-nm band ( $\epsilon > 1000 \text{ M}^{-1} \text{cm}^{-1}$ ) and an  $R_{\text{abs}} \geq 0.20$  have rhombic EPR spectra.

What is the structural basis for increased rhombicity in EPR spectra and enhanced absorptivity at 460 nm? From single-crystal studies of plastocyanin and a model compound, Gewirth et al.<sup>65</sup> suggested that the rhombic distortion was due to a strengthening of the Cu–X(axial ligand) bond. Thus, axial EPR character should be associated with a trigonal-planar Cu–NNS site. Rhombic EPR character should be associated with movement of the Cu away from the NNS plane, generating a more tetrahedral coordination geometry. This hypothesis is supported by a comparison of the properties of wild-type *A. denitrificans* azurin and the M121Q mutant in which the axial methionine ligand has been replaced by a glutamine (coordinated to copper through the amide carbonyl group).<sup>54</sup> The M121Q mutant has a rhombic rather than axial EPR spectrum as well as increased absorbance at 460 nm, and the crystal structure

(62) (a) Chang, T. K.; Iverson, S. A.; Rodrigues, C. G.; Kiser, C. N.; Lew, A. Y. C.; Germanas, J. P.; Richards, J. H. *Proc. Natl. Acad. Sci. U.S.A.* **1991**, *88*, 1325–1329. (b) Dave, B. P.; Germanas, J. P.; Czernuszewicz, R. S. Personal communication.

(63) Knapp, S.; Keenan, T. P.; Zhang, X.; Fikar, R.; Potenza, J. A.; Schugar, H. J. *J. Am. Chem. Soc.* **1990**, *112*, 3452–3464.

(64) Larrabee, J. A.; Spiro, T. G. *J. Am. Chem. Soc.* **1980**, *102*, 4217–4223.

(65) Gewirth, A. A.; Cohen, S. L.; Schugar, H. J.; Solomon, E. I. *Inorg. Chem.* **1987**, *26*, 1133–1146.

indicates that the Cu has moved out of the NNS plane by 0.26 Å compared to 0.12 Å in wild-type (Table II).

The other crystallographic data in Table II also support the correlation between EPR rhombicity and a strengthening of the Cu–X(axial ligand) bond. Thus, short Cu–S(Met) distances (<2.8 Å) are observed for the rhombic sites in pseudoazurin, cucumber basic protein, and nitrite reductase. Longer Cu–S(Met) distances are observed for the axial sites in azurin (3.13 Å) and plastocyanin<sup>66</sup> from *Enteromorpha prolifera* (2.92 Å). Although the Cu–S(Met) distance of 2.82 Å for *Populus nigra* plastocyanin (Table II) is somewhat borderline, the uncertainty in Cu–ligand bond distances is  $\pm 0.05$  Å even in high-resolution protein crystal structures.<sup>3</sup> The Cu···(NNS) distances listed in Table II are more variable, but do indicate a trend toward longer distances in the rhombic category. Thus, the high 460-nm absorbance of rhombic type 1 Cu sites is most likely due to stronger coordination of the axial ligand.

The changes in the alignment of copper and sulfur orbitals associated with the conversion from trigonal-planar to a tetrahedral geometry would be expected to affect absorption energies as well as intensities. This is indeed observed (Table II). The proteins in the axial EPR category have their average absorption maxima at 462 and 603 nm, whereas those in the rhombic EPR category have their average absorption maxima at 452 and 598 nm. Similar trends are apparent in the set of Met 121 ligand mutants from *P.a* azurin.<sup>61</sup> Replacement of Met 121 with Leu, Ala, Thr, Val, Ile, or Trp yields an axial EPR spectrum consistent with weak or absent axial ligation and a trigonal-planar geometry. This group has  $R_{\text{abs}}$  values ranging from 0.09 to 0.15 and average absorption maxima at 460 and 625 nm. Replacement of Met 121 with Asn, Asp, Gln, Cys, or His yields a rhombic EPR spectrum consistent with stronger axial ligation and a more tetrahedral geometry. The  $R_{\text{abs}}$  values for this group range from 0.15 to 0.48 and the average absorption maxima are at 450 and 610 nm. Thus, increased energies for the Cu–cysteinate electronic transitions are yet another indicator of tetrahedral character in type 1 copper proteins.

(66) Collyer, C. A.; Guss, J. M.; Sugimura, Y.; Yoshizaki, F.; Freeman, H. C. *J. Mol. Biol.* **1990**, *211*, 617–632.

## Conclusions

1. The RR spectra of NiR and mutant SOD (H80C) are typical of type 1 Cu sites, indicating that both have a short Cu–S(Cys) bond of  $\sim 2.1$  Å. The large number of vibrational modes between 340 and 415  $\text{cm}^{-1}$  is due, in part, to the kinematic coupling of  $\nu(\text{Cu–S})$  with Cys deformation modes and is, thus, indicative of a coplanar cysteine.

2. In the electronic spectra,  $\epsilon_{460}$  varies from 300  $\text{M}^{-1} \text{cm}^{-1}$  in plastocyanin to 1180 in pseudoazurin and 2530 in NiR, while the  $\epsilon_{600}$  varies from 5200  $\text{M}^{-1} \text{cm}^{-1}$  in plastocyanin to 2900 in pseudoazurin and 1890 in NiR. This inverse relationship in  $\epsilon$  values suggests that a common chromophoric group may be responsible for the two electronic transitions.

3. The 460- and the 600-nm electronic transitions give rise to the same RR frequencies and, thus, can be ascribed to the same Cu–cysteinate ground-state structure. Their variable Raman intensities require different excited-state structures. Both absorptions are likely to have substantial (Cys)S  $\rightarrow$  Cu(II) CT character.

4. Increased intensity at 460 nm and increased rhombicity in the EPR spectrum both appear to be correlated with a more tetrahedral site where the Cu has moved away from the NNS ligand plane and toward the axial ligand.

5. Since the 460- and 600-nm copper–cysteinate transitions are observed in the electronic spectra of all type 1 Cu proteins, the definition of a type 1 Cu site should be expanded to include the occurrence of two absorption bands at 460 and 600 nm.

**Acknowledgment.** We are grateful to Drs. Edward I. Solomon and Michael D. Lowery for helpful discussions of the electronic spectra. We thank Drs. Elinor T. Adman and Gerard W. Canters for providing X-ray structural information for nitrite reductase and the M121Q azurin mutant, respectively, prior to publication. We also thank Drs. Michael Jackson and Eduardo Libby for preparation of nitrite reductase. This research was supported by the National Institutes of Health, Grants GM 18865 (T.M.L., J.S.-L.) and GM 28222 (J.S.V.), and the National Science Foundation, Grant DMB-8917427 (B.A.A.).